13th Australasian Fluid Mechanics Conference
Monash University, Melbourne, Australia
13-18 December 1998

NUMERICAL PREDICTIONS OF FORCES ON A LONG RECTANGULAR PLATE SUBJECTED TO CROSS-FLOW PERTURBATION

Boon T. TAN, Mark C. THOMPSON and Kerry HOURIGAN

Department of Mechanical Engineering
Monash University, Clayton, Victoria, AUSTRALIA

ABSTRACT

Numerical predictions of the standard deviation of lift and mean drag force are presented for rectangular cross-sectioned plates with aspect ratios $(c/t) = 6 - 16$. The simulations are at $Re = 400$ and the plates are subjected to a sinusoidal oscillation with an amplitude of 2.5% of free-stream velocity in the frequency range of $0.1 < St < 0.2$. The peaks in drag force with varying c/t display a stepwise increase in St_c suggesting that the response is dominated by an *Impinging Leading-Edge Vortex* (ILEV) instability. Overall the fluctuating component of lift shows an increase with frequency but decreases close to these frequencies at which the drag is a maximum.

NOMENCLATURE

c	plate chord
$\overline{C_D}$	time average drag coefficient
C_L	lift coefficient
c/t	Chord to thickness ratio
Re	Reynolds number
St	Strouhal number based on thickness
St_c	Strouhal number based on chord
t	plate thickness
v	magnitude of cross-flow perturbation
ϕ	Phase angle of sinusoidal forcing
σ_{C_L}	standard deviation of lift coefficient

INTRODUCTION

In many industrial applications, it is important to quantify the loading on bluff bodies in fluid-structure interactions. For flow past long rectangular plates, there is a complex interaction between leading and trailing edge vortex shedding. The receptivity of the instability can be measured by introducing a small oscillatory perturbation to the system. A long rectangular plate sheds vortices from both the leading edge and trailing edge and is susceptible to a feedback type of instability. High aspect ratio bodies experience increased fluctuating lift which can result in structural instability.

The flow under investigation is shown in Figure 1. The two-dimensional long rectangular plate is placed

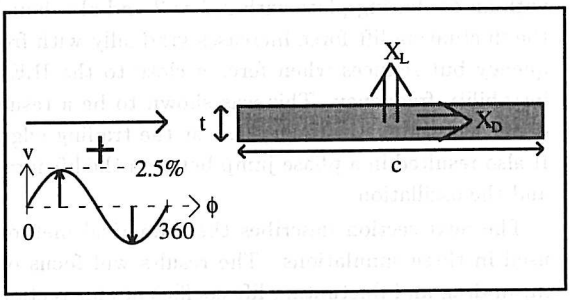

Figure 1: Physical layout of the simulation.

in a uniform flow with a sinusoidal cross-flow perturbation of 2.5% of the free stream velocity.

In the unforced case, this impinging shear layer instability or ILEV instability (Naudascher and Rockwell, 1994) locks the flow to distinct periodic shedding modes. Experiments by Nakamura *et al.* (1991) at $Re = 1,000$ for $c/t = 3 - 15$ showed that the leading edge shedding locks on so that there is an integer mode of shedding corresponding to a discrete number of vortices on the plate. This resulted in a step wise increase in St_c with plate length. Ozono *et al.* (1992) and Ohya *et al.* (1992) demonstrated the same stepping with numerical simulations at $Re = 1,000$ for $c/t = 3 - 9$.

At higher Reynolds number this feedback mechanism is weak and the flow will not lock into distinct shedding modes without some external excitation. Stokes and Welsh (1986) ($Re = 15,000 - 30,000$) enclosed the plate in a duct and found that when the frequency of the acoustic field generated by the plate in the duct is near the instability frequency, it locks the shedding. Mills *et al.* (1995) ($Re = 9,000$) applied acoustic forcing to the plate and found that the base pressure peaks also display a stepwise increase with c/t.

A comparison of the time-averaged base pressure measurements of Mills *et al.* (1995) and the predicted pressures from the method used in this paper is presented in Tan *et al.* (1998). The instability manifested itself in both cases with peaks in base pressure corresponding to the different shedding modes. The applied frequency at which the base suction is a max-

imum depends on the phase difference between the leading edge vortices passing the trailing edge and the forcing. Besides the gradual increase in base suction as the forcing frequency approaches the critical frequency, the applied perturbation also leads to a shorter re-attachment length at the leading edge and an increased spanwise correlation, base suction and circulation of vortices in the wake.(Stokes and Welsh, 1986, Hourigan *et al.*, 1993, Mills *et al.*, 1995).

Blackburn and Henderson (1996) and Blackburn and Karniadakis (1993) showed that for both free and forced oscillating cylinders, the drag force increased, and the fluctuating lift force decreased, near the critical frequency. Deniz and Staubli (1997) experimented with an oscillating plate with $c/t = 2$ and also found the fluctuating lift force increases gradually with frequency but reduces when forcing close to the ILEV instability frequency. This was shown to be a result of the change in shedding phase at the trailing edge. It also resulted in a phase jump between the lift force and the oscillation.

The next section describes the numerical method used in these simulations. The results will focus on mean drag and fluctuating lift coefficients for rectangular plates with $6 < c/t < 16$ showing the effects of the (impinging leading edge vortex) instability. All simulations presented are performed at $Re = 400$. Results for a preliminary three-dimensional simulation for the natural shedding case will also be presented.

NUMERICAL METHOD

The governing equations are the incompressible Navier-Stokes equations in primitive variables.

Spatial Scheme

The spectral-element method has been used for the computations. This method can be characterised as a high-order Galerkin finite-element method with tensor-product Lagrange polynomials used to interpolate the fields in each element. For smooth problems, this method allows high-order spatial accuracy to be achieved. For this geometry (a rectangular plate) the right angle corners of the plate restrict the spatial convergence rate of the method, however, the effect is local and does not degrade the accuracy of the flow-field away from these points.

The boundary conditions applied to the computational domain are, (i) no slip on the plate, (ii) zero normal velocity derivative at the outflow boundary and, (iii) on the side and inflow boundary, the velocity was taken as uniform in the horizontal direction plus a perturbing sinusoidally varying vertical component.

Figure 2 shows a typical mesh system used for the simulations. This mesh is for a plate with chord to thickness ratio of 10. It employs 7×7 nodes per

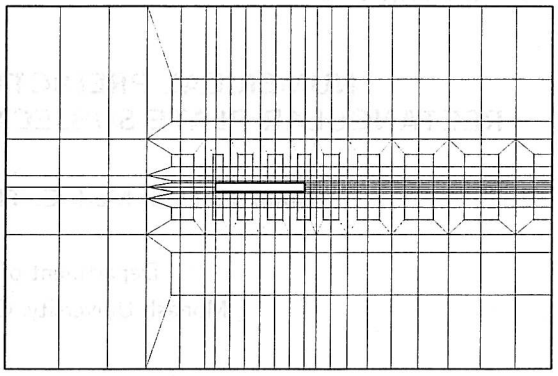

Figure 2: Computational grid showing only macro-elements for $c/t = 10$. Each macro-element contains 49 nodes.

element, *i.e.*, 6th order Lagrangian polynomials in each direction. The outflow boundary is placed $28t$ downstream from the trailing edge of the plate and the side boundaries $20t$ plate thicknesses away from the plate. Tests with larger domains indicate that these dimensions are adequate to predict pressures on the plate to within approximately 3%. Drag and lift coefficients are normalised with respect to t and c respectively.

Temporal Scheme

The implementation employs the classical three-step splitting scheme for the time stepping as described in Karniadakis *et al.* (1991). Each time-step is split into three sub-steps to treat the advection, mass conservation/pressure and diffusion terms of the Navier-Stokes equations. The Navier-Stokes equations are discretised in conservative form which leads to discrete energy conservation. The pressure and implicit viscous sub-steps result in linear matrix problems. The matrices are not a function of time and so only need to be inverted once at the beginning of the calculations. Subsequently these steps only involve a (sparse) matrix multiplication. The non-linear term has to be treated explicitly. Typically this is done using the third-order Adam-Bashforth scheme. The temporal derivatives from the viscous sub-step are treated using the Crank-Nicolson method. Higher-order boundary conditions are applied to the pressure sub-step to ensure at least second-order overall time accuracy for the velocity field. The time step is restricted by the Courant condition, and set at 0.007 dimensionless time units which is less than 1/700th of a period. The computational results were analysed only after the flow had reached an asymptotic state as determined by monitoring the base pressure variation with time. Typically this requires 20 to 30 shedding cycles.

Accuracy

A limited number of simulations were performed at a higher resolution. For the $c/t = 10$ several simula-

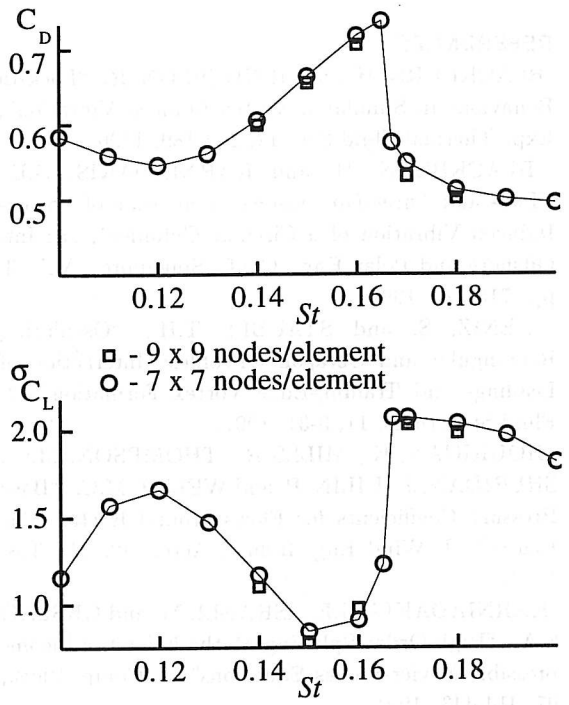

Figure 3: Comparison mean drag and standard deviation of lift coefficient as a function of forcing frequency for $c/t = 10$ at different resolutions.

tions were performed using the same grid with 9×9 noded elements. Increasing the order of the element also increases the total number of nodes and results in a more severe Courant restriction. The time step used was 0.004 dimensionless time units. Results presented in Figure 3 show that increasing the spatial resolution and reducing the time step does not significantly alter the prediction. This suggests that the simulations are well resolved.

RESULTS

For the aspect ratios used in these simulations, the shedding locked to the forcing over a wide range of frequency, typically between $0.10 < St < 0.22$. Calculated values of time average drag and standard deviation of lift will be presented for $c/t = 6 - 16$ and for $0.10 < St < 0.20$.

Drag Force

The mean drag force coefficients are presented in Figure 4. The St at which the mean drag force peaks decreases with increasing c/t. The flow will then lock into a higher mode of shedding and the pattern repeats. This pattern is highlighted by the long dashed lines in Figure 4 and is characteristic of the *Impinging Leading-Edge Vortex Instability*(ILEV). Also the drag is larger for plates that peak around $St = 0.15$ and decreases for peaks further away. This behaviour is consistent with base pressure measurements presented by Mills *et al.* (1995) and predicted by Tan *et al.* (1998).

Lift Force

The standard deviation of lift coefficient is presented in Figure 5. The general trend is that the fluctuating component of lift increases with frequency and aspect ratio. The instability that causes peaks in base pressure result in a decrease in fluctuating lift. The long dashed lines in Figure 5 connecting the local minima in fluctuating lift also display a similar trend to mean drag force suggesting the influence of the same instability.

Comparison with Three Dimensional Simulation

Some preliminary results have been obtained for three dimensional simulations for this geometry without the perturbations. These simulations were carried out using the same parameters but with a span of $2\pi t$ and a Fourier expansion in the spanwise direction resulting in a periodic boundary condition. The results for the two aspect ratios investigated so far are tabulated in Table 1.

c/t	σ_{C_L}		$\overline{C_D}$	
	2D	3D	2D	3D
10	0.0716	0.0377	0.820	0.705
13	0.0388	0.0185	0.711	0.658

Table 1: Comparison of lift and drag forces for two and three dimensional simulations.

Flow Visualisation

Vorticity plots for the aspect ratio $c/t = 14$ are shown in Figure 6. The forcing frequency is chosen to correspond to the frequency that results in maximum mean drag and a reduced fluctuating lift force ($St = 0.155$). Two other frequencies just below and above this are included for comparison ($St = 0.14$ and $St = 0.17$). The plots are taken at two instances in the forcing cycle (0 deg and 90 deg).

At the same phase in the forcing, the shedding from the leading edge is in phase with the forcing frequency independent of frequency. These vortices travel downstream and lock the phase of the trailing-edge shedding resulting in a varying phase of shedding from the trailing-edge with forcing frequency. Closer to the ILEV instability frequency, the increase in drag can be attributed to stronger shedding from the trailing-edge and a reduction in the formation length. At higher frequencies, the trailing edge shedding is suppressed and undergoes a phase shift of approximately 180^o.

Also included in Figure 6 is a plot of pressure along the top and bottom surfaces of the plate. The pressure plots for the three frequencies are not significantly different. Below the vortices there is an increase in suction on the plate and the effects decays as the vortices convect downstream.

DISCUSSION

The impinging shear layer instability influences both lift and drag forces. The magnitude of the peaks in mean drag force vary with c/t but give larger values closer to $St = 0.15$. The fluctuations in lift force do not mirror this feature. The St at which the instability is strongest only occur at the same phase condition for the different aspect ratios (Mills *et al.*, 1995, Tan *et al.*, 1998). As a large contribution to the drag force is from the trailing-edge (since the drag force from the leading edge is approximately constant), it is hypothesised that the receptivity of the trailing edge is stronger closer to that frequency.

The forcing locks the leading-edge shedding. At higher frequencies, there are more discrete vortices along the plate resulting in a gradual increase in lift with forcing frequency. Superimposed on this is a gradual rise in fluctuating lift forces at frequencies just below and above the frequency at which it reaches a local minimum. This is consistent with the cylinder and the short plate(Blackburn and Karniadakis, 1993, Deniz and Staubli, 1997).

A comparison of the two and three dimensional force calculation show that the fluctuating lift component is much higher in the two-dimensional case. This is due to the three-dimensionality of the flow on the plate, namely *Pattern B* (Kiya and Sasaki 1991), reducing the span-wise correlation. The mean drag is similar in both simulations. The flow around the front face of the plate is two dimensional. Although the three-dimensional structures on the surface of the plate convect downstream, the trailing edge shedding is still predominantly two dimensional at this Reynolds number leading to a similar drag force for both cases. However, this may not be the case at higher Re, when the three-dimensionality is much stronger.

CONCLUSION

The mean drag and fluctuating lift for long rectangular plates is governed by the *Impinging Leading-Edge Vortex* (ILEV) instability. At the ILEV instability frequency, the mean drag increases and the fluctuating lift decreases. The increase in drag is due to stronger vortices forming at the trailing edge and and a reduction in formation length. The fluctuating lift force increases with frequency because of an increasing number of vortices along the plate. At the ILEV instability frequency, there is a reduction in fluctuating lift.

ACKNOWLEDGEMENTS

The first author would like to acknowledge the financial support of the Monash Postgraduate Scholarship and Overseas Postgraduate Research Scholarship. The Monash High Performance Computing facility made the simulations in this paper possible.

REFERENCES

BLACKBURN, H. and HENDERSON, R., "Lock-In Behaviour in Simulated Vortex-Induced Vibration", Exp. Thermal Fluid Sci., 12, 184-189, 1996.

BLACKBURN, H. and KARNIADAKIS, G.E., "Two- and Three-Dimensional Simulation of Vortex-Induced Vibration of a Circular Cylinder", 3rd Int. Offshore and Polar Eng. Conf., Singapore , Vol. 3, pp. 715-720, 1993.

DENIZ, S. and STAUBLI, T.H., "Oscillating Rectangular and Octagonal Profiles: Interaction of Leading- and Trailing-Edge Vortex Formation", J. Fluid Structures, 11, 3-31, 1997.

HOURIGAN, K., MILLS R., THOMPSON, M.C., SHERIDAN, J., DILIN, P. and WELSH, M.C., "Base Pressure Coefficients for Flows around Rectangular Plates.", J. Wind Eng. Indust. Aero., 49, 311–318, 1993.

KARNIADAKIS, G.E., ISRAELI, M. and ORSZAG S.A., "High-Order Splitting Methods for the Incompressible Navier-Stokes Equations", J. Comp. Phys., 97, 414-443. 1991.

MILLS, R., SHERIDAN, J., HOURIGAN, K. and WELSH, M.C., "The Mechanism Controlling Vortex Shedding from Rectangular Bluff Bodies", Proceedings of the 12th Australasian Fluid Mechanics Conference, 227-230, Sydney, December 1995.

NAKAMURA, Y., OHYA, Y., and TSURUTA, H., "Experiments on Vortex Shedding from Flat Plates with Square Leading Edges", J. Fluid Mech, 222, 437-447, 1991.

OZONO, S., OHYA, Y., NAKAMURA, Y. and NAKAYAMA, R., "Stepwise Increase in the Strouhal Number for Flows around Flat Plates", Int. J. Num. Methods Fluids, 15, 1025-1036, 1992.

OHYA, Y., NAKAMURA, Y., OZONO, S., TSURUTA, H. and NAKAYAMA, R., "A Numerical Study of Vortex Shedding from Flat Plates with Square Leading and Trailing Edges", J. Fluid Mech., 236, 445-460, 1992.

NAUDASCHER, E. and ROCKWELL, D., "Flow-Induced Vibration - An Engineering Guide", Rotterdam : A.A. Balkema, 1994.

SASAKI, K. and KIYA, M., "Three-dimensional Vortex Structure in a Leading Edge Separation Bubble at Moderate Reynolds Number", J. Fluids Eng., 113, 405-410, 1991.

STOKES, A. N. and WELSH, M.C., "Flow-Resonant Sound Interaction in a Duct Containing a Plate, II: Square Leading Edge", J. Sound and Vibration, 104, 55-73, 1986.

TAN, B. T., THOMPSON, M.C. and HOURIGAN K., "Simulation of Perturbed Flow Around a Rectangular Cylinder ", Proceedings of the ASME Fluids Engineering Division Summer Meeting, Pap. no. 5166, Washington, June 1998.